Since January 2020 Elsevier has created a COVID-19 resource centre with free information in English and Mandarin on the novel coronavirus COVID-19. The COVID-19 resource centre is hosted on Elsevier Connect, the company's public news and information website.

Journal Pre-proofs

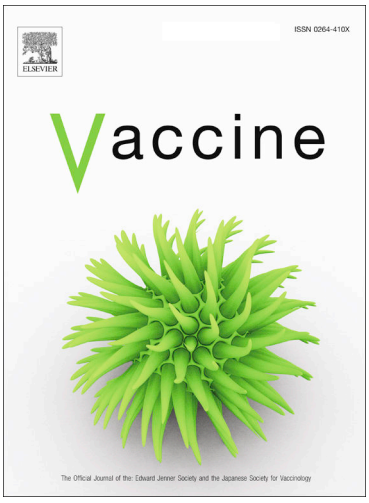

PD-1/PD-L1 blockade restores tumor-induced COVID-19 vaccine bluntness

Xiangyu Chen, Yao Lin, Shuai Yue, Yang Yang, Xiaofan Yang, Junjian He, Leiqiong Gao, Zhirong Li, Li Hu, Jianfang Tang, Yifei Wang, Qin Tian, Yaxing Hao, Lifan Xu, Qizhao Huang, Yingjiao Cao, Lilin Ye

PII: S0264-410X(23)00737-5
DOI: https://doi.org/10.1016/j.vaccine.2023.06.053
Reference: JVAC 25085

To appear in: *Vaccine*

Received Date: 28 January 2023
Revised Date: 14 May 2023
Accepted Date: 15 June 2023

Please cite this article as: X. Chen, Y. Lin, S. Yue, Y. Yang, X. Yang, J. He, L. Gao, Z. Li, L. Hu, J. Tang, Y. Wang, Q. Tian, Y. Hao, L. Xu, Q. Huang, Y. Cao, L. Ye, PD-1/PD-L1 blockade restores tumor-induced COVID-19 vaccine bluntness, *Vaccine* (2023), doi: https://doi.org/10.1016/j.vaccine.2023.06.053

PD-1/PD-L1 blockade restores tumor-induced COVID-19 vaccine bluntness

Xiangyu Chen[a,1], Yao Lin[b,1], Shuai Yue[b,c,1], Yang Yang[d,1], Xiaofan Yang[e], Junjian He[b], Leiqiong Gao[b], Zhirong Li[b], Li Hu[b], Jianfang Tang[b], Yifei Wang[d], Qin Tian[e], Yaxing Hao[b], Lifan Xu[b], Qizhao Huang[d], Yingjiao Cao[d,*] and Lilin Ye[a,b,d,*]

[a]School of Basic Medical Sciences, Southern Medical University, Guangzhou, 510515, China.

[b]Institute of Immunology, Third Military Medical University, Chongqing, 400038, China.

[c]Cancer Center, Daping Hospital & Army Medical Center of PLA, Third Military Medical University, Chongqing, 400042, China.

[d]Guangdong Provincial Key Laboratory of Immune Regulation and Immunotherapy, School of Laboratory Medicine and Biotechnology, Southern Medical University, Guangzhou, 510515, China.

[e]Dermatology Hospital, Southern Medical University, Guangzhou, 510091, China.

[1]These authors contributed equally to this work.

*Corresponding authors. E-mail addresses: cyj20120703@163.com (Yingjiao Cao) and yelilinlcmv@tmmu.edu.cn (Lilin Ye).

Highlights

- Antibody response to COVID-19 vaccination is largely impaired during malignancy.
- Tumor-induced COVID-19 vaccine bluntness is associated with poor follicular helper T cell and B cell responses.
- The tumor-suppressed COVID-19 vaccine effectiveness is restored by PD-1/PD-L1 blockade.
- PD-1/PD-L1 blockade preferentially preserves follicular helper T cell response during malignancy.
- The PD-1/PD-L1 blockade-recovered COVID-19 vaccine effectiveness is independent of anti-tumor therapeutic outcomes.

Abstract

The COVID-19 vaccinations are crucial in protecting against the global pandemic. However, accumulating studies revealed the severely blunted COVID-19 vaccine effectiveness in cancer patients. The PD-1/PD-L1 immune checkpoint blockade (ICB) therapy leads to durable therapeutic responses in a subset of cancer patients and has been approved to treat a wide spectrum of cancers in the clinic. In this regard, it is pivotal to explore the potential impact of PD-1/PD-L1 ICB therapy on COVID-19 vaccine effectiveness during ongoing malignancy. In this study, using preclinical models, we found that the tumor-suppressed COVID-19 vaccine responses are largely reverted in the setting of PD-1/PD-L1 ICB therapy. We also identified that the PD-1/PD-L1 blockade-directed restoration of COVID-19 vaccine effectiveness is irrelevant to anti-tumor therapeutic outcomes. Mechanistically, the restored COVID-19 vaccine effectiveness is entwined with the PD-1/PD-L1 blockade-driven preponderance of follicular helper T cell and germinal center responses during ongoing malignancy. Thus, our findings indicate that PD-1/PD-L1 blockade will greatly normalize the responses of cancer patients to COVID-19 vaccination, while regardless of its anti-tumor efficacies on these patients.

Keywords

COVID-19 vaccine, SARS-CoV-2 RBD, T_{FH} cell, PD-1/PD-L1 blockade, Cancer immunotherapy

1. Introduction

During the global pandemic of coronavirus disease 2019 (COVID-19), cancer patients are reported to be at higher risk of being infected by SARS-CoV-2 and developing more severe COVID-19 disease [1, 2], thus prioritizing cancer patients for COVID-19 vaccinations. However, accumulating evidence indicated that patients of both solid and hematologic malignancies poorly respond to currently used COVID-19 vaccines, including BNT162b2 mRNA vaccine, mRNA-1273 vaccine and ChAdOx1 nCoV-19 vaccine [3-7].

The compromised COVID-19 vaccine efficacies in cancer patients might be attributed to multiple factors, including the underlying malignancy itself, cytotoxic chemotherapy-associated bone marrow suppressive effects and, especially, the immunosuppressive activities of cancer therapeutics [8]. Indeed, COVID-19 vaccine responses are severely blunted in cancer patients receiving antibody therapies (e.g., anti-CD20 antibody, anti-CD38 antibody) [3, 4, 8, 9], targeted therapies (e.g., Bruton tyrosine kinase inhibitors (BTKi), B cell lymphoma 2 inhibitors (Bcl-2i), CDK4/6 inhibitors) [3, 8] and chimeric antigen receptor (CAR)-T therapies [8]. Nevertheless, the impacts of immune checkpoint inhibitors, as exemplified by PD-1/PD-L1 immune checkpoint blockade (ICB) therapy, on the COVID-19 vaccine responses of cancer patients are less well understood.

PD-1/PD-L1 ICB therapy has elicited durable clinical responses in a certain fraction of cancer patients and thus revolutionized the cancer treatment regimen [10]. One crucial mechanism underlying PD-1/PD-L1 ICB therapy-directed tumor regression is the reinvigoration of exhausted tumor antigen-specific $CD8^+$ T cells with abundant PD-1 expression [11, 12]. In addition to exhausted $CD8^+$ T cells, PD-1 is also highly expressed by follicular helper T (T_{FH}) cells that specifically promote B cell-mediated humoral responses to infection and vaccination [13, 14]. In this regard, understanding COVID-19 vaccine response in the scenario of PD-1/PD-L1 ICB therapy will provide important insights into the COVID-19 vaccine regimen of cancer patients. Herein, we explored the effects of both effectual and failed PD-1/PD-L1 ICB therapy in motoring COVID-19 vaccine effectiveness in mouse models. Furthermore, the underlying cellular mechanisms of COVID-19 vaccine response to PD-1/PD-L1 ICB therapy were also investigated.

2. Materials and methods

2.1. Mice

C57BL/6 and $CD45.1^+$ congenic (strain B6.SJL-*Ptprc*^{a} *Pepc*^{b}/BoyJ) mice were purchased from the Jackson Laboratories. Smarta transgenic (carrying a transgenic T cell antigen receptor that recognizes I-A^b GP_{66-77} epitope) mice were gifts from Dr. Rafi Ahmed (Emory University). All the mice used in the study were analyzed at 6-10 weeks of age, and both genders were included without randomization or blinding. All mice used in the study were carried out in accordance with procedures approved by the Institutional Animal Care and Use Committees of Third Military Medical University.

2.2. Immunization schedule

For COVID-19 vaccination, C57BL/6 mice were immunized with 2 dosages of COVID-19 vaccines via intramuscular route into the anterolateral aspect of the right thigh in an interval of 10 days. The priming COVID-19 vaccine contains 5 μg SARS-CoV-2 prototype RBD proteins (Sino Biological, 40592-V08H) and 10 μg CpG ODN 1826 adjuvant (Invitrogen), while the booster COVID-19 vaccine contains 5 μg SARS-CoV-2 Omicron (B.1.1.529) RBD proteins (Sino Biological, 40592-V08H122) and 10 μg CpG ODN 1826 adjuvant (Invitrogen). For LCMV GP_{61-80} peptide vaccination, C57BL/6 mice were intramuscularly injected with 2 dosages of 10 μg LCMV GP_{61-80} peptide and 10 μg CpG ODN 1826 adjuvant (Invitrogen), spaced 10 days apart. At day 2-post the first LCMV GP_{61-80} peptide vaccination, a total of 2×10^5 SM cells were intravenously injected into immunized C57BL/6 mice.

2.3. Tumor models

MC38 cells and B16F10 cells were purchased from ATCC and cultured in complete DMEM-10 medium (Gibco) supplied with 10% FBS (Gibco), 1% penicillin/streptomycin (Gibco), and 1% L-glutamine (Gibco). C57BL/6 mice were subcutaneously implanted with 2×10^5 MC38 cells or 2×10^5 B16F10 cells at the anterolateral aspect of the left thigh. Tumor volumes were measured with a caliper and calculated according to the formula: ((length × $width^2$)/2). Tumor-engrafted mice were sacrificed at indicated timepoints on the premise of the humane endpoints (tumor volume not exceeding 2,000 mm^3). For anti-PD-L1 antibody treatment experiments, mice were intraperitoneally injected with 200 μg anti-PD-L1 antibody (BioXcell, clone 10F.9G2) at indicated time points.

2.4. Enzyme-linked immunosorbent assay (ELISA)

The ELISA plates (Thermo Fisher, 446469) were coated with 50 ng SARS-CoV-2 prototype RBD proteins (Sino Biological, 40592-V08H) or 50 ng SARS-CoV-2 Omicron (B.1.1.529) RBD proteins (Sino Biological, 40592-V08H122) or 1 μg LCMV GP_{61-80} peptide in 100 μl PBS per well overnight. On the next day, the ELISA plates were first performed with 1-hour incubation of blocking buffer (5% FBS + 0.1% Tween 20 in PBS). Then, 10-fold serially diluted mouse sera were added to each well and incubated for 1 hour. Next, the ELISA plates were successively washed with PBST (PBS + 0.1% Tween 20), incubated with HRP-conjugated goat anti-mouse IgG antibody (Bioss Biotech), washed with PBST and added with TMB (Beyotime). The ELISA plates were performed with ~5 min reaction with TMB and stopped by 1 M H_2SO_4 stop buffer. The optical density (OD) value was determined at 450 nm.

2.5. SARS-CoV-2 pseudovirus neutralization assay

SARS-CoV-2 pseudovirus neutralization assays were performed as previously described [15]. Briefly, SARS-CoV-2 pseudotyped particles were produced by co-transfecting 293T cells with psPAX2, pLenti-luciferase, and plasmids encoding SARS-CoV-2 prototype spike or SARS-CoV-2 Omicron spike at a ratio of 1:1:1. After 48 hours, the supernatants containing SARS-CoV-2 pseudovirus were harvested. SARS-CoV-2 pseudotyped particles, including prototype strain and the Omicron strain, were pre-incubated with 3-fold serially diluted mouse sera for 1 hour at 37ºC. Then, hACE2-expressing HEK-293T (hACE2/293T) cells were incubated with the sera/pseudovirus mixtures overnight and then cultured with fresh complete DMEM-10 medium. At 48 hours post incubation, the luciferase activities of SARS-CoV-2 typed pseudovirus-infected hACE2/293T cell lysates were determined by a luciferase reporter assay kit (Promega, E1910). NT50 was determined by using four-parameter logistic regression.

2.6. Flow cytometry

Lymphocytes of the vaccine-dLNs and spleens were harvested by mashing the tissues through cell strainer (BD Falcon). Antibodies for flow cytometry analysis in the study include CD4 (Biolegend, clone RM4-5), CD45.1 (Biolegend, clone A20), PD-1 (Biolegend, clone 29F.1A12), CD44 (eBioscience, clone IM7), B220 (Biolegend, clone), CD19 (Biolegend, clone 1D3/CD19), FAS (BD Biosciences, clone Jo2), PNA (Vector Labs, clone FL-1071), Bcl-6 (BD Biosciences, clone K112-91) and FoxP3 (eBioscience, clone FJK-16s). Stainings of cell surface markers were performed in PBS containing 2% FBS. Staining for CXCR5 was described previously[16]. Briefly, cells were successively stained with purified anti-CXCR5 (BD Biosciences) for 1 hour at 4ºC, biotinylated anti-rat IgG (Jackson Immunoresearch) for 30 min on ice and fluorescent-dye conjugated streptavidin (Thermo Fisher) for 30 min on ice. Stainings for FoxP3 and Bcl-6 were performed with the Foxp3/Transcription Factor Staining Buffer Set (eBioscience, 00-5523). Dead cells were stained using LIVE/DEAD Fixable Near-IR Dead Cell Stain Kit (Life Technologies). Flow cytometry data were acquired in a FACSCanto II (BD Biosciences) or a FACSFortesa (BD Biosciences) and analyzed using FlowJo.

2.7. Statistical analysis

Statistical analyses were performed with Prism 9.0 (GraphPad). One-way ANOVA with Newman-Keul's test was used for comparisons. Graphs show individual samples and center values indicate mean. *P* values less than 0.05 were defined as statistically significant. **P* < 0.05, ***P* < 0.01, ****P* < 0.001 and *****P* < 0.0001.

3. Results

3.1. Effective PD-1/PD-L1 ICB therapy restores tumor-induced blunted antibody responses to COVID-19 vaccination

To ascertain the effects of PD-1/PD-L1 ICB therapy on antibody responses of specificity to COVID-19 vaccination, naïve C57BL/6 mice were subcutaneously engrafted with syngeneic MC38 colon adenocarcinoma cells and then prime/boost immunized with 2 dosages of SARS-CoV-2 receptor binding domain (RBD) protein, a core part of COVID-19 vaccines [17, 18], based subunit vaccine with CpG as adjuvant. Specifically, mice were immunized with SARS-CoV-2 prototype RBD protein and Omicron B.1.1.529 (hereinafter referred to as Omicron) RBD protein at day 3- and day 13-post tumor engraftment, respectively. During tumorigenesis, a total 6 injections of anti-PD-L1 antibodies were administrated every 3 days from day 6 to day 21 (Fig. 1A). As expected, PD-L1 ICB-directed remarkable tumor regression was observed in MC38 tumors with a trait of high sensitivity to PD-1/PD-L1 blockade (Fig. 1B). As controls, naïve C57BL/6 mice without MC38 tumor engraftment were prime/boost immunized with SARS-CoV-2 RBD proteins in the presence or absence of anti-PD-L1 antibody administrations (Fig. 1A).

On day 10 after priming immunization, sera were collected from mice of each group and performed with enzyme-linked immunosorbent assay (ELISA) to examine IgG antibodies that specifically bind to SARS-CoV-2 prototype RBD. Consistent with published studies in cancer patients [3-7], MC38 tumor burden severely impaired the titers of IgG antibodies specific to SARS-CoV-2 prototype RBD in mice (Fig. 1C and Fig. S1A). Notably, tumor burden-mediated blunted SARS-CoV-2 RBD-specific IgG antibody titers were almost completely rescued by PD-L1 blockade (Fig. 1C and Fig. S1A). Parallelly, we found no reinforcements of SARS-CoV-2 RBD-specific IgG antibody titers in anti-PD-L1 antibody-treated control mice without tumor engraftment (Fig. 1C and Fig. S1A). Therefore, PD-1/PD-L1 ICB therapy unleashes tumor-suppressed antibody responses post-prime COVID-19 vaccination.

Next, we harvested sera on day 10 after boosted COVID-19 vaccination and determined SARS-CoV-2 RBD-specific IgG antibodies by ELISA. Consistently, IgG antibody titers to both SARS-CoV-2 prototype and Omicron RBDs were blunted by tumor burden. And such bluntness was reverted upon anti-PD-L1 antibody treatment (Fig. 1D, E and Fig. S1B, C). Importantly, the total IgG antibody levels were comparable among all the groups (Fig. S2A), indicating the specific suppression of tumor burden on vaccine-induced antibody responses. To exclude the potential suboptimal vaccine efficacy of heterogenous SARS-CoV-2 RBD immunization in generating prototype- or Omicron-specific antibody responses, we measured the serum IgG antibodies specifically binding to prototype RBD in MC38 tumor-engrafted mice receiving 2 dosages of prototype RBD immunization (Fig. S3A, B). Likewise, MC38 tumor severely impaired the titers of IgG antibodies specific to SARS-CoV-2 prototype RBD, while tumor-mediated blunted SARS-CoV-2 RBD-specific IgG antibody titers were completely rescued by PD-L1 blockade in the scenario of

prototype RBD prime-boost immunization (Fig. S3C).

To further determine the quantity of neutralizing antibodies generated in each condition, we accessed the neutralizing activities of these collected sera by pseudovirus neutralization assays as previously described [19-21]. In line with published studies [3, 5], serum neutralizing capacity against SARS-CoV-2 prototype and Omicron variants was compromised in the presence of tumor burden (Fig. 1F, G). Importantly, PD-L1 blockade rectified serum neutralizing capacity against SARS-CoV-2 variants in tumor-engrafted mice (Fig. 1F, G). Thus, these findings illuminate that PD-1/PD-L1 ICB therapy dramatically restores the blunted antibody responses to COVID-19 vaccination in tumor-engrafted mice.

3.2. Tumor burden-impaired SARS-CoV-2 RBD-specific B cell responses are rebounded upon PD-1/PD-L1 ICB therapy

Given that memory B cells instigate antigen-specific antibodies and predict anamnestic responses after booster vaccination [22], we next examined B cell responses in the vaccine-draining lymph nodes (dLNs) of mice in each condition on day 23 post-tumor engraftment as described in Fig. 1A. First, we noted that both frequency and number of B cells were restrained in tumor-engrafted mice relative to the control mice and such restraints were counterbalanced by PD-L1 ICB therapy (Fig. 2A-C). Then, we investigated antigen-specific B cells marked by avidin-tagged biotinylated SARS-CoV-2 RBD antigen bait as previously described [23, 24]. Alarmingly, we found that frequencies and numbers of B cells specific to both SARS-CoV-2 prototype and Omicron RBDs were largely diminished in the presence of tumor burden (Fig. 2D-I), echoing the poor quality and quantity of SARS-CoV-2 RBD-specific antibody in tumor-engrafted mice (Fig. 1). The SARS-CoV-2 RBD-specific B cell responses were rebounded upon PD-L1 ICB therapy (Fig. 2D-I), which might reflect the cellular mechanisms underlying the recovered antibody responses to SARS-CoV-2 RBD in tumor-engrafted mice treated with anti-PD-L1 antibodies.

Germinal center (GC) B cells are the important source of the highly neutralizing antibodies for protective immunity [25]. We then analyzed the polyclonal GC B cells, as indicated by co-expression of FAS and PNA, in the vaccine-dLNs of mice in each group. Interestingly, we observed an increased frequency of GC B cells in tumor-engrafted group as compared the other groups (Fig. 2J, K), which might be due to the survival bias of GC B cell as reported in other study [26]. Nonetheless, the total number of GC B cells was decreased in tumor-engrafted mice and rescued by PD-L1 antibody treatment (Fig. 2L). Overall, these results depict the rebounded B cell responses to SARS-CoV-2 RBD immunization that aligned with PD-1/PD-L1 ICB therapy in tumor-engrafted mice.

3.3. PD-1/PD-L1 ICB therapy promotes T_{FH} cell responses to COVID-19 vaccination in the context of tumor burden

Considering the specialized and critical role of T_{FH} cells in promoting the class switching and hypermutation of cognate B cells in GC [14], we next examined T_{FH} cell responses in vaccine-dLNs of aforementioned SARS-CoV-2 RBD-immunized mice in each condition. Likewise, we found T_{FH} cells in vaccine-dLNs were quantitatively constrained by tumor burden (Fig. 3A-C). And such quantitative straits of T_{FH} cells were also relieved in the situation of PD-L1 ICB therapy (Fig. 3A-C), which rationalizes the unleashed B cell responses in tumor-engrafted mice receiving anti-PD-L1 treatment.

PD-1 is highly expressed by GC T_{FH} cells due to the long-term TCR signaling from cognate B cells in GC [13]. We found that blocking PD-1/PD-L1 signaling amplifies GC T_{FH} cell differentiation, as exemplified by increased PD-1^{hi} T_{FH} cell frequency as well as enhanced PD-1 protein expressions, in both control and tumor-engrafted mice receiving anti-PD-L1 antibody treatment (Fig. 3D-F). Nevertheless, the total GC T_{FH} cell responses were not reinforced in control group treated with anti-PD-L1 antibodies, but completely rescued in tumor-engrafted group with PD-L1 ICB therapy (Fig. 3G), which highlights the contribution of PD-1/PD-L1 ICB therapy in restoring GC T_{FH} cell responses in the scenario of tumor burden.

T follicular regulatory (T_{FR}) cells are an effector subset of $CD4^+FoxP3^+$ regulatory T (T_{reg}) cells that specifically controls GC responses by suppressing T_{FH}-B cell interaction [27]. Resembling T_{FH} cells, we found that both T_{reg} and T_{FR} cells in vaccine-dLNs are quantitatively compromised in tumor-engrafted group (Fig. 3H-J and Fig. S4). Reportedly, T_{FR} cells are characterized by the abundant PD-1 expression and show enhanced suppressive function in the deficiency of PD-1/PD-L1 signaling [28]. Indeed, we found that the compression of T_{FR} cells in tumor-engrafted mice is rescued by PD-L1 ICB therapy (Fig. 3H-J). The PD-1 protein expressions in T_{FR} cells were also increased in the presence of PD-L1 ICB therapy, albeit with lower enhancement as compared to those observed in PD-L1 antibody-treated T_{FH} cells (Fig. 3K, L). Given that T_{FH} cell to T_{FR} cell ratio is a crucial proxy to gauge the GC responses [27], we next determined this parameter in each group. Importantly, we noticed the highest T_{FH} cell to T_{FR} cell ratio in tumor-engrafted group with PD-L1 ICB therapy (Fig. 3M, N), indicating the preponderance of strengthened T_{FH} cell response compared to T_{FR} cell response upon PD-L1 ICB therapy in the presence of tumor burden. Together, these findings support the notion that COVID-19 vaccine-induced T_{FH} cell responses are preserved by PD-L1 ICB therapy in the context of ongoing malignancy.

3.4. Viral antigen-specific GC T_{FH} cell responses are restored by PD-1/PD-L1 ICB therapy in tumor-engrafted mice

To more precisely track antigen-specific GC T_{FH} cell responses in the situation of PD-1/PD-L1 ICB therapy-directed tumor regression, naïve C57BL/6 mice were firstly subcutaneously engrafted with syngeneic MC38 colon adenocarcinoma cells and then received adoptive transfer of $CD45.1^+$ congenic smarta (SM) $CD4^+$ T cells recognizing lymphocytic choriomeningitis virus (LCMV) glycoprotein (GP) epitope I-$A^b$$GP_{66-77}$ at day 2 after tumor engraftment. These recipients were next prime/boost immunized with LCMV GP_{61-80}

peptide in an interval of 10 days and administrated with 6 injections of anti-PD-L1 as described (Fig. 4A). Parallelly, control groups without MC38 tumor engraftment were administrated following the same procedure (Fig. 4A). Expectedly, anti-PD-L1 antibody treatment effectively shrank the tumor burden (Fig. 4B) and refurbished tumor-suppressed LCMV GP_{61-80}-specific antibody responses (Fig. 4C) and B cell responses (Fig. S5).

We next investigated viral antigen-specific $CD4^+$ T cells by tracking transferred $CD45.1^+$ SM cells in vaccine-dLNs and spleens. Analogously, SM cell responses in both vaccine-dLNs and spleens were restricted by tumor burden and such restriction was unleashed by PD-L1 ICB therapy (Fig. 4D, E and Fig. S6A, B). Furthermore, antigen-specific GC T_{FH} cell responses, as indicated by co-expression of CXCR5, PD-1 and Bcl-6 [13, 14], were poorly mounted during tumor progression (Fig. 4F-J and Fig. S6C-F). Of particular importance was the reinvigoration of antigen-specific GC T_{FH} cell responses in tumor-engrafted mice receiving PD-L1 ICB therapy (Fig. 4F-J and Fig. S6E, F). Taken together, these findings suggest that vaccine-induced antigen-specific GC T_{FH} cell responses are crashed by tumor burden and re-endowed with PD-L1 ICB therapy in tumor-engrafted mice.

3.5. PD-1/PD-L1 blockade also reinvigorates tumor-blunted COVID-19 vaccine response in ICB-resistant tumor-engrafted mice

Though PD-1/PD-L1 ICB therapy mediates durable remissions in a subset of cancer patients [29, 30], its response rates remain modest in some cancer types [31] (e.g., melanoma and breast cancer) and even inert in cancer types such as glioblastoma [32]. We therefore specifically asked the COVID-19 vaccine response in the scenario of ineffective or failed PD-1/PD-L1 ICB tumor immunotherapy. Towards this end, naïve C57BL/6 mice were subcutaneously engrafted with PD-L1/PD-1 ICB therapy-resistant B16F10 melanoma cells and then prime/boost immunized with SARS-CoV-2 prototype and Omicron RBDs at day 3 and day 13, respectively, after tumor engraftment (Fig. 5A). In concert with published studies [33, 34], B16F10 melanoma completely resisted PD-L1 ICB therapy (Fig. 5B), albeit a total 6 injections of anti-PD-L1 antibodies were administrated as described (Fig. 5A). Next, we set out to examine SARS-CoV-2 RBD-specific antibody responses in the scenario of ineffectual PD-L1 ICB therapy. In line with aforementioned data in MC38 tumor model, SARS-CoV-2 RBD-specific antibody titers were also restricted by B16F10 tumor burden (Fig. 5C, D), with B cell and T_{FH} cell responses concurrently being suppressed (Fig. 5E-G). More notably, we found that B16F10 tumor-blunted antibody responses to COVID-19 vaccine are averted by PD-L1 ICB therapy (Fig. 5C, D), in spite of no tumor regression (Fig. 5B). Such restoration might be attributed to the preserved T_{FH}-B cell responses upon anti-PD-L1 antibody treatment (Fig. 5E-G). Therefore, these observations demonstrate that PD-1/PD-L1 ICB therapy is able to effectively rectify vaccine-induced antibody responses in hosts with ICB-non-responsive tumor.

4. Discussion

Accumulated studies reported the poor COVID-19 vaccine responses in cancer patients [3-7]. Herein, in line with these studies, we also observed the blunted COVID-19 vaccine effectiveness in both murine colon carcinoma and melanoma models. Importantly, we found that PD-1/PD-L1 ICB therapy robustly restores the COVID-19 vaccine effectiveness, irrespective of the tumor regression rate to PD-1/PD-L1 ICB therapy. Furthermore, we unraveled evidence suggesting the restoration of COVID-19 vaccine response is mainly tied to the T_{FH}-B cell interaction preserved by PD-1/PD-L1 ICB therapy in tumor-engrafted mice.

In response to vaccination, T_{FH} cells are crucial in providing essential assistance to B cells and thus promoting GC responses in B cell follicles within secondary lymphoid tissues. The GC responses entails rapid production of high-affinity antibodies for immediate protection and generation of memory B cells for long-term protection [13, 14]. One important feature of T_{FH} cells is heightened PD-1 protein that control T_{FH} cell positioning and function [35]. Reportedly, T_{FH} cells deficient in PD-1 signaling show enhanced follicular recruitment; however, the antibody affinity maturation is compromised in the absence of PD-1 signaling due to decreased stringency of GC affinity selection [35]. Consistently, another study observed that cancer patients receiving PD-1 ICB therapy have more robust circulating T_{FH} cells and resultant higher antibody titer to influenza vaccination than healthy participants not receiving PD-1 ICB therapy; however, the affinity of influenza-specific antibody is decreased in the setting of PD-1 ICB therapy [36]. In the study, we also noted strengthened T_{FH} cell responses and resultant enhanced antibody response to COVID-19 vaccination in tumor-engrafted mice receiving PD-L1 ICB therapy. Noticeably, the PD-L1 blockade-reinforced antibody response, in spite of potential low affinity, is recovered from tumor-suppressive nadir level and shows comparable neutralizing capacity to that of healthy controls. Therefore, the animal data here suggests that PD-L1 ICB therapy might benefit COVID-19 vaccine response in the scenario of ongoing malignancy, which awaits further clinical validations.

Another potential cellular mechanism contributing to the PD-1/PD-L1 ICB therapy-directed reinvigoration of COVID-19 vaccine response during ongoing malignancy is the proliferating preponderance of T_{FH} cells relative to T_{FR} cells. Though T_{FR} cells were reported to show proliferating burst and enhanced suppressive effects to GC responses in the deficiency of PD-1 signaling [28], the T_{FR} cell reactivity might be compensated by the PD-1/PD-L1-directed bias for T_{FH} cell response to COVID-19 vaccination during ongoing malignancy. This notion is further supported by the observed T_{FH} cell expansion in cancer patients post-PD-1/PD-L1 ICB therapy in other studies [36-38]. Moreover, decreased circulating T_{FR} cells were even found in cancer patients concurrently receiving influenza vaccination and anti-PD-1 antibodies [36]. The potential reasons for the PD-1/PD-L1 blockade-mediated superior response of T_{FH} cells relative to T_{FR} cells include 1) highly-sensitivity of T_{FH} cells to PD-1/PD-L1 blockade in the setting of ongoing malignancy and 2) less tumor-associated suppression to T_{FH} cells. These hypotheses need to be further investigated.

Previous studies [39, 40], including our own [41], indicated that tumor-associated suppressive effects on $CD8^+$ T cell responses against infections and vaccinations. Related to this, we further identified evidence of tumor-associated suppression on GC responses, as indicated by largely compromised T_{FH} cell and B cell responses to COVID-19 vaccination in tumor-engrafted mice. This point is further evidenced by the partially recovered COVID-19 vaccine effectiveness in cancer patients with surgery therapy [8]. The potential mechanisms underlying tumor-associated suppressive effects on T_{FH} cells and B cells might be tumor burden-driven expansion of immunosuppressive immune cells, including erythroid progenitor cells [41] and neutrophils [42], and tumor burden-induced perturbations in dendritic cells [39]. Besides, tumor-derived exosomes might also be involved in suppressing T_{FH} cell and B cell responses to COVID-19 vaccination [43]. Nevertheless, given the restored COVID-19 vaccine effectiveness in both settings of effectual and failed PD-L1 ICB therapy in tumor-engrafted mice, we concluded that the PD-L1 ICB therapy-directed re-sharpness of COVID-19 vaccine responses in tumor-engrafted mice might be mainly attributed to the GC responses strengthened by PD-1/PD-L1 signaling blockade *per se* rather than durable tumor regression driven by PD-L1 ICB therapy. Therefore, it seems that PD-1/PD-L1 ICB therapy also benefits the COVID-19 vaccine effectiveness in cancer patients without durable clinical outcomes.

To date, the effects of PD-1/PD-L1 ICB therapy on COVID-19 vaccine response of cancer patients have been reported in several clinical studies, albeit with debatable conclusions. On the one hand, comparable antibody responses against COVID-19 vaccination were observed between cancer patients with PD-1/PD-L1 ICB therapy and healthy participates [44, 45], which hints the restoration of tumor-blunted COVID-19 vaccine effectiveness in patients receiving PD-1/PD-L1 ICB therapy to that of healthy participates. Indeed, cancer patients with PD-1/PD-L1 ICB therapy showed a trend towards increased COVID-19 vaccine effectiveness as compared to that of cancer patients with no therapies [5, 46]. Otherwise, several studies reported lower COVID-19 vaccine-induced antibody responses in cancer patients receiving PD-1/PD-L1 ICB therapy relative to healthy participants [47, 48]. And such discrepancy might be attributed to missed experimental control of cancer patients without any therapies or different regimen of COVID-19 vaccination and PD-1/PD-L1 ICB therapy. Here, we provided clear evidence of reinforced COVID-19 vaccine effectiveness during ongoing malignancy with multiple mouse models, which reconciles the discrepancies in aforementioned clinical studies and provides guidance for related clinical investigations in the future.

This study has some limitations. First, more COVID-19 vaccine platforms (e.g., mRNA vaccines, viral vector-based vaccines) should be involved in the study. Second, the molecular mechanisms underlying PD-L1 blockade-driven reinforcement of B cell and T_{FH} cell responses are unknown. These issues are worthy of further investigations.

5. Conclusions

In conclusion, we demonstrated that PD-1/PD-L1 ICB therapy reinvigorates COVID-19

vaccine effectiveness in mice with ongoing malignancy. And such reinvigoration is highly associated with strengthened GC responses in the absence of PD-1-PD-L1 interaction. Therefore, our findings unravel the COVID-19 vaccine response in the setting of PD-1/PD-L1 ICB therapy and suggest that COVID-19 vaccines combined with PD-1/PD-L1 blockade might be administrated to cancer patients to improve the protection from SARS-CoV-2 infection, even if PD-1/PD-L1 ICB therapy may fail to control the tumor progression.

Data availability

The data in the study are available from the corresponding authors upon reasonable request.

Acknowledgments

This work was supported by grants from the National Natural Science Foundation of China (No. 31900642 to Y.H.), the National Natural Science Fund for Distinguished Young Scholars (No. 31825011 to L.Y.) and the National Science and Technology Major Project (No. 2017ZX10202102-006-002 to L.Y.).

Author contributions

X.C., Y.L., S.Y., and Y.Y. performed the experiments. Z.L., L.H. and J.T. assisted in preparing experimental regents. X.Y., J.H., L.G., Y.W., Q.T., Y.H., L.X. and Q.H. helped to discuss the results; X.C. designed the study, analyzed the data and drafted the paper with L.Y. and Y.C.; and L.Y. supervised the study.

Declaration of Competing Interest

The authors declare no competing interests.

References

[1] Dai M, Liu D, Liu M, Zhou F, Li G, Chen Z, et al. Patients with Cancer Appear More Vulnerable to SARS-CoV-2: A Multicenter Study during the COVID-19 Outbreak. Cancer Discov. 2020;10:783-91.

[2] Kuderer NM, Choueiri TK, Shah DP, Shyr Y, Rubinstein SM, Rivera DR, et al. Clinical impact of COVID-19 on patients with cancer (CCC19): a cohort study. Lancet.

2020;395:1907-18.

[3] Chang A, Akhtar A, Linderman SL, Lai L, Orellana-Noia VM, Valanparambil R, et al. Humoral Responses Against SARS-CoV-2 and Variants of Concern After mRNA Vaccines in Patients With Non-Hodgkin Lymphoma and Chronic Lymphocytic Leukemia. J Clin Oncol. 2022;40:3020-31.

[4] Keppler-Hafkemeyer A, Greil C, Wratil PR, Shoumariyeh K, Stern M, Hafkemeyer A, et al. Potent high-avidity neutralizing antibodies and T cell responses after COVID-19 vaccination in individuals with B cell lymphoma and multiple myeloma. Nat Cancer. 2022.

[5] Valanparambil RM, Carlisle J, Linderman SL, Akthar A, Millett RL, Lai L, et al. Antibody Response to COVID-19 mRNA Vaccine in Patients With Lung Cancer After Primary Immunization and Booster: Reactivity to the SARS-CoV-2 WT Virus and Omicron Variant. J Clin Oncol. 2022:Jco2102986.

[6] Massarweh A, Eliakim-Raz N, Stemmer A, Levy-Barda A, Yust-Katz S, Zer A, et al. Evaluation of Seropositivity Following BNT162b2 Messenger RNA Vaccination for SARS-CoV-2 in Patients Undergoing Treatment for Cancer. JAMA Oncol. 2021;7:1133-40.

[7] Shroff RT, Chalasani P, Wei R, Pennington D, Quirk G, Schoenle MV, et al. Immune responses to two and three doses of the BNT162b2 mRNA vaccine in adults with solid tumors. Nat Med. 2021;27:2002-11.

[8] Thakkar A, Gonzalez-Lugo JD, Goradia N, Gali R, Shapiro LC, Pradhan K, et al. Seroconversion rates following COVID-19 vaccination among patients with cancer. Cancer Cell. 2021;39:1081-90.e2.

[9] Fendler A, Shepherd STC, Au L, Wilkinson KA, Wu M, Byrne F, et al. Adaptive immunity and neutralizing antibodies against SARS-CoV-2 variants of concern following vaccination in patients with cancer: The CAPTURE study. Nat Cancer. 2021;2:1321-37.

[10] Sharma P, Allison JP. The future of immune checkpoint therapy. Science. 2015;348:56-61.

[11] Sharma P, Allison JP. Dissecting the mechanisms of immune checkpoint therapy. Nat Rev Immunol. 2020;20:75-6.

[12] McLane LM, Abdel-Hakeem MS, Wherry EJ. CD8 T Cell Exhaustion During Chronic Viral Infection and Cancer. Annu Rev Immunol. 2019;37:457-95.

[13] Crotty S. Follicular helper CD4 T cells (TFH). Annu Rev Immunol. 2011;29:621-63.

[14] Crotty S. T Follicular Helper Cell Biology: A Decade of Discovery and Diseases. Immunity. 2019;50:1132-48.

[15] Ou X, Liu Y, Lei X, Li P, Mi D, Ren L, et al. Characterization of spike glycoprotein of

SARS-CoV-2 on virus entry and its immune cross-reactivity with SARS-CoV. Nat Commun. 2020;11:1620.

[16] Li R, Pan Z, Wu J, Yue S, Lin Y, Yang Y, et al. The Epigenetic Regulator EZH2 Instructs CD4 T Cell Response to Acute Viral Infection via Coupling of Cell Expansion and Metabolic Fitness. J Virol. 2020;94.

[17] Yang J, Wang W, Chen Z, Lu S, Yang F, Bi Z, et al. A vaccine targeting the RBD of the S protein of SARS-CoV-2 induces protective immunity. Nature. 2020;586:572-7.

[18] Wang Q, Zhang Y, Wu L, Niu S, Song C, Zhang Z, et al. Structural and Functional Basis of SARS-CoV-2 Entry by Using Human ACE2. Cell. 2020;181:894-904.e9.

[19] Chen X, Pan Z, Yue S, Yu F, Zhang J, Yang Y, et al. Disease severity dictates SARS-CoV-2-specific neutralizing antibody responses in COVID-19. Signal Transduct Target Ther. 2020;5:180.

[20] Lin Y, Yue S, Yang Y, Yang S, Pan Z, Yang X, et al. Nasal Spray of Neutralizing Monoclonal Antibody 35B5 Confers Potential Prophylaxis Against Severe Acute Respiratory Syndrome Coronavirus 2 (SARS-CoV-2) Variants of Concern (VOCs): A Small-scale Clinical Trial. Clin Infect Dis. 2022.

[21] Wang X, Chen X, Tan J, Yue S, Zhou R, Xu Y, et al. 35B5 antibody potently neutralizes SARS-CoV-2 Omicron by disrupting the N-glycan switch via a conserved spike epitope. Cell host & microbe. 2022;30:887-95.e4.

[22] Sette A, Crotty S. Adaptive immunity to SARS-CoV-2 and COVID-19. Cell. 2021;184:861-80.

[23] Chen X, Li R, Pan Z, Qian C, Yang Y, You R, et al. Human monoclonal antibodies block the binding of SARS-CoV-2 spike protein to angiotensin converting enzyme 2 receptor. Cell Mol Immunol. 2020;17:647-9.

[24] Wang X, Hu A, Chen X, Zhang Y, Yu F, Yue S, et al. A potent human monoclonal antibody with pan-neutralizing activities directly dislocates S trimer of SARS-CoV-2 through binding both up and down forms of RBD. Signal Transduct Target Ther. 2022;7:114.

[25] Young C, Brink R. The unique biology of germinal center B cells. Immunity. 2021;54:1652-64.

[26] Mesin L, Ersching J, Victora GD. Germinal Center B Cell Dynamics. Immunity. 2016;45:471-82.

[27] Sage PT, Sharpe AH. T follicular regulatory cells in the regulation of B cell responses. Trends Immunol. 2015;36:410-8.

[28] Sage PT, Francisco LM, Carman CV, Sharpe AH. The receptor PD-1 controls follicular

regulatory T cells in the lymph nodes and blood. Nat Immunol. 2013;14:152-61.

[29] Brahmer JR, Tykodi SS, Chow LQ, Hwu WJ, Topalian SL, Hwu P, et al. Safety and activity of anti-PD-L1 antibody in patients with advanced cancer. The New England journal of medicine. 2012;366:2455-65.

[30] Topalian SL, Hodi FS, Brahmer JR, Gettinger SN, Smith DC, McDermott DF, et al. Safety, activity, and immune correlates of anti-PD-1 antibody in cancer. The New England journal of medicine. 2012;366:2443-54.

[31] Nishino M, Ramaiya NH, Hatabu H, Hodi FS. Monitoring immune-checkpoint blockade: response evaluation and biomarker development. Nat Rev Clin Oncol. 2017;14:655-68.

[32] Chamberlain MC, Kim BT. Nivolumab for patients with recurrent glioblastoma progressing on bevacizumab: a retrospective case series. Journal of neuro-oncology. 2017;133:561-9.

[33] Garris CS, Arlauckas SP, Kohler RH, Trefny MP, Garren S, Piot C, et al. Successful Anti-PD-1 Cancer Immunotherapy Requires T Cell-Dendritic Cell Crosstalk Involving the Cytokines IFN-γ and IL-12. Immunity. 2018;49:1148-61.e7.

[34] Ahern E, Harjunpää H, O'Donnell JS, Allen S, Dougall WC, Teng MWL, et al. RANKL blockade improves efficacy of PD1-PD-L1 blockade or dual PD1-PD-L1 and CTLA4 blockade in mouse models of cancer. Oncoimmunology. 2018;7:e1431088.

[35] Shi J, Hou S, Fang Q, Liu X, Liu X, Qi H. PD-1 Controls Follicular T Helper Cell Positioning and Function. Immunity. 2018;49:264-74.e4.

[36] Herati RS, Knorr DA, Vella LA, Silva LV, Chilukuri L, Apostolidis SA, et al. PD-1 directed immunotherapy alters Tfh and humoral immune responses to seasonal influenza vaccine. Nat Immunol. 2022;23:1183-92.

[37] Satpathy AT, Granja JM, Yost KE, Qi Y, Meschi F, McDermott GP, et al. Massively parallel single-cell chromatin landscapes of human immune cell development and intratumoral T cell exhaustion. Nat Biotechnol. 2019;37:925-36.

[38] Bassez A, Vos H, Van Dyck L, Floris G, Arijs I, Desmedt C, et al. A single-cell map of intratumoral changes during anti-PD1 treatment of patients with breast cancer. Nat Med. 2021;27:820-32.

[39] Allen BM, Hiam KJ, Burnett CE, Venida A, DeBarge R, Tenvooren I, et al. Systemic dysfunction and plasticity of the immune macroenvironment in cancer models. Nat Med. 2020;26:1125-34.

[40] van der Burg SH, Arens R, Ossendorp F, van Hall T, Melief CJ. Vaccines for established cancer: overcoming the challenges posed by immune evasion. Nat Rev Cancer. 2016;16:219-33.

[41] Zhao L, He R, Long H, Guo B, Jia Q, Qin D, et al. Late-stage tumors induce anemia and immunosuppressive extramedullary erythroid progenitor cells. Nat Med. 2018;24:1536-44.

[42] Hiam-Galvez KJ, Allen BM, Spitzer MH. Systemic immunity in cancer. Nat Rev Cancer. 2021;21:345-59.

[43] Whiteside TL. Exosomes and tumor-mediated immune suppression. J Clin Invest. 2016;126:1216-23.

[44] Felip E, Pradenas E, Romeo M, Marfil S, Trinité B, Urrea V, et al. Impact of chemotherapy and/or immunotherapy on neutralizing antibody response to SARS-CoV-2 mRNA-1237 vaccine in patients with solid tumors. Mol Oncol. 2022.

[45] Oosting SF, van der Veldt AAM, GeurtsvanKessel CH, Fehrmann RSN, van Binnendijk RS, Dingemans AC, et al. mRNA-1273 COVID-19 vaccination in patients receiving chemotherapy, immunotherapy, or chemoimmunotherapy for solid tumours: a prospective, multicentre, non-inferiority trial. Lancet Oncol. 2021;22:1681-91.

[46] Niewolik J, Mikuteit M, Cossmann A, Vahldiek K, Gutzmer R, Müller F, et al. Immunogenicity of COVID-19 Vaccination in Melanoma Patients under Immune Checkpoint Blockade. Oncology. 2022;100:392-8.

[47] Terpos E, Liontos M, Fiste O, Zagouri F, Briasoulis A, Sklirou AD, et al. SARS-CoV-2 Neutralizing Antibodies Kinetics Postvaccination in Cancer Patients under Treatment with Immune Checkpoint Inhibition. Cancers (Basel). 2022;14.

[48] Terpos E, Zagouri F, Liontos M, Sklirou AD, Koutsoukos K, Markellos C, et al. Low titers of SARS-CoV-2 neutralizing antibodies after first vaccination dose in cancer patients receiving checkpoint inhibitors. J Hematol Oncol. 2021;14:86.

Figure legends

Fig. 1. Effective PD-1/PD-L1 ICB therapy restores tumor-induced blunted antibody responses to COVID-19 vaccination. A. Schematic graph of the experiment design. **B.** MC38 tumor growth curve of mice with or without anti-PD-L1 antibody treatment. **C.** ELISA binding assay of sera collected from mice at 10 days-post prime vaccination to SARS-CoV-2 prototype RBD. **D, E.** ELISA binding assays of sera collected from mice at 10 days-post boost vaccination to SARS-CoV-2 prototype RBD (**D**) and Omicron RBD (**E**). **F, G.** Neutralization of sera collected from mice at 10 days-post boost vaccination to SARS-CoV-2 prototype (**F**) and Omicron (**G**) variants. AUC, area under curve. NT50, neutralizing titer 50. ns, not significant. **P* < 0.05 and ***P* < 0.01. The data are representative of two independent experiments with five to six mice per group. Error bars (B-G) indicate s.e.m..

Fig. 2. Tumor burden-impaired SARS-CoV-2 RBD-specific B cell responses are rebounded upon PD-1/PD-L1 ICB therapy. A. Flow cytometry analysis of lymphocytes in vaccine-dLNs. The numbers adjacent to the outlined areas indicate the percentages of $CD19^+B220^+$ B cells. **B, C.** Frequency (**B**) and number (**C**) of B cells in vaccine-dLNs. **D.** Flow cytometry analysis of $CD19^+B220^+$ B cells in vaccine-dLNs. The numbers adjacent to the outlined areas indicate the percentages of SARS-CoV-2 prototype RBD-specific B cells. **E, F.** Frequency (**E**) and number (**F**) of SARS-CoV-2 prototype RBD-specific B cells in vaccine-dLNs. **G.** Flow cytometry analysis of $CD19^+B220^+$ B cells in vaccine-dLNs. The numbers adjacent to the outlined areas indicate the percentages of SARS-CoV-2 Omicron RBD-specific B cells. **H, I.** Frequency (**H**) and number (**I**) of SARS-CoV-2 Omicron RBD-specific B cells in vaccine-dLNs. **J.** Flow cytometry analysis of $CD19^+B220^+$ B cells in vaccine-dLNs. The numbers adjacent to the outlined areas indicate the percentages of FAS^+PNA^+ GC B cells. **K, L.** Frequency (**K**) and number (**L**) of FAS^+PNA^+ GC B cells in vaccine-dLNs. ns, not significant. **P* < 0.05, ***P* < 0.01 and ****P* < 0.001. The data are representative of two independent experiments with five mice per group. Error bars (B, C, E, F, H, I, K, L) indicate s.e.m..

Fig. 3. PD-1/PD-L1 ICB therapy promotes T_{FH} cell responses to COVID-19 vaccination in the context of tumor burden. A. Flow cytometry analysis of $CD4^+FoxP3^-$ T cells in vaccine-dLNs. The numbers adjacent to the outlined areas indicate the percentages of $CXCR5^+CD44^{hi}$ T_{FH} cells. **B, C.** Frequency (**B**) and number (**C**) of T_{FH} cells in vaccine-dLNs. **D.** Flow cytometry analysis of $CXCR5^+CD44^{hi}$ T_{FH} cells in vaccine-dLNs. The numbers adjacent to the outlined areas indicate the percentages of PD-1^{hi} T_{FH} cells. **E-G.** Frequency (**E**), PD-1 protein level (**F**) and number (**G**) of PD-1^{hi} T_{FH} cells in vaccine-dLNs. **H.** Flow cytometry analysis of $CD4^+FoxP3^+$ T cells in vaccine-dLNs. The numbers adjacent to the outlined areas indicate the percentages of $CXCR5^+$ T_{FR} cells. **I, J.** Frequency (**I**) and number (**J**) of T_{FR} cells in vaccine-dLNs. **K.** Frequency of PD-1^{hi} T_{FR} cells. **L.** PD-1 protein

level of PD-1^{hi} T_{FR} cells. **M.** T_{FH} cell to T_{FR} cell ratio in vaccine-dLNs. **N.** PD-1^{hi} T_{FH} cell to PD-1^{hi} T_{FR} cell ratio in vaccine-dLNs. MFI, mean fluorescence intensity. ns, not significant. **P* < 0.05, ***P* < 0.01, ****P* < 0.001 and *****P* < 0.0001. The data are representative of two independent experiments with five mice per group. Error bars (B, C, E-G, I-N) indicate s.e.m..

Fig. 4. Viral antigen-specific GC T_{FH} cell responses are restored by PD-1/PD-L1 ICB therapy in tumor-engrafted mice. A. Schematic graph of the experiment design. **B.** MC38 tumor growth curve of mice with or without anti-PD-L1 antibody treatment. **C.** ELISA binding assay of sera collected from mice at 10 days-post boost vaccination to LCMV GP_{61-80} peptide. **D, E.** Frequency (**D**) and number (**E**) of transferred CD45.1^{+} SM cells in spleens. **F.** Flow cytometry analysis of transferred CD45.1^{+} SM cells in spleens. The numbers adjacent to the outlined areas indicate the percentages of CXCR5^{+}PD-1^{hi} GC T_{FH} cells. **G, H.** Frequency (**G**) and number (**H**) of transferred PD-1^{hi} SM T_{FH} cells in spleens. **I, J.** Frequency (**I**) and number (**J**) of transferred Bcl-6^{hi} SM T_{FH} cells in spleens. ns, not significant. **P* < 0.05, ***P* < 0.01 and ****P* < 0.001. The data are representative of two independent experiments with six mice per group. Error bars (B-E, G-J) indicate s.e.m..

Fig. 5. PD-1/PD-L1 blockade also reinvigorates tumor-blunted COVID-19 vaccine response in ICB-resistant tumor-engrafted mice. A. Schematic graph of the experiment design. **B.** B16F10 tumor growth curve of mice with or without anti-PD-L1 antibody treatment. **C, D.** ELISA binding assay of sera collected from mice at 10 days-post boost vaccination to SARS-CoV-2 prototype RBD (**C**) and Omicron RBD (**D**). **E-F.** Numbers of B cells (**E**), GC B cells (**F**) and T_{FH} cells (**G**) in vaccine-dLNs. ns, not significant. **P* < 0.05 and ***P* < 0.01. The data are representative of two independent experiments with six mice per group. Error bars (B-G) indicate s.e.m..

Declaration of interests

☒ The authors declare that they have no known competing financial interests or personal relationships that could have appeared to influence the work reported in this paper.

□ The authors declare the following financial interests/personal relationships which may be considered as potential competing interests:

Figure 1

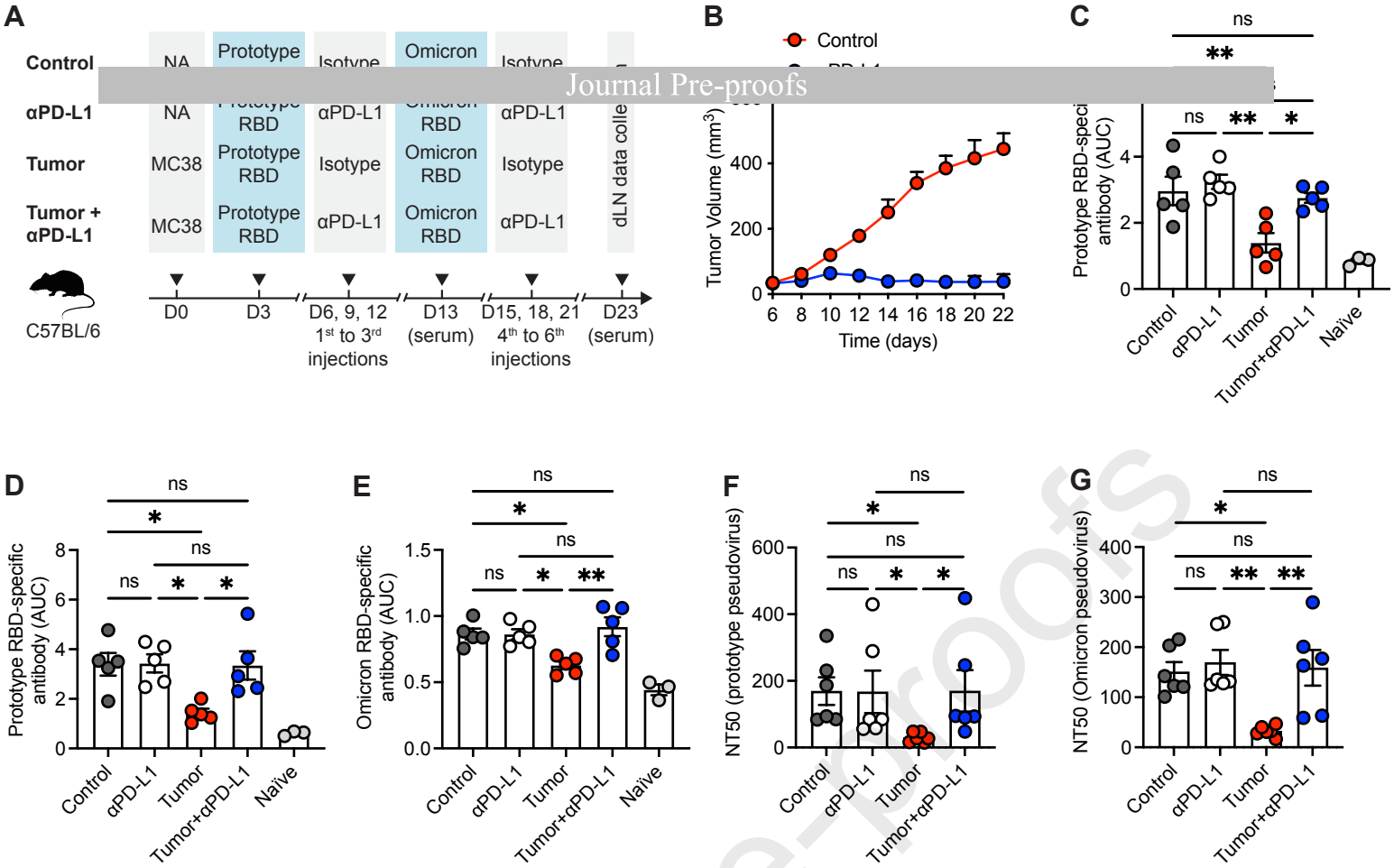

Figure 2

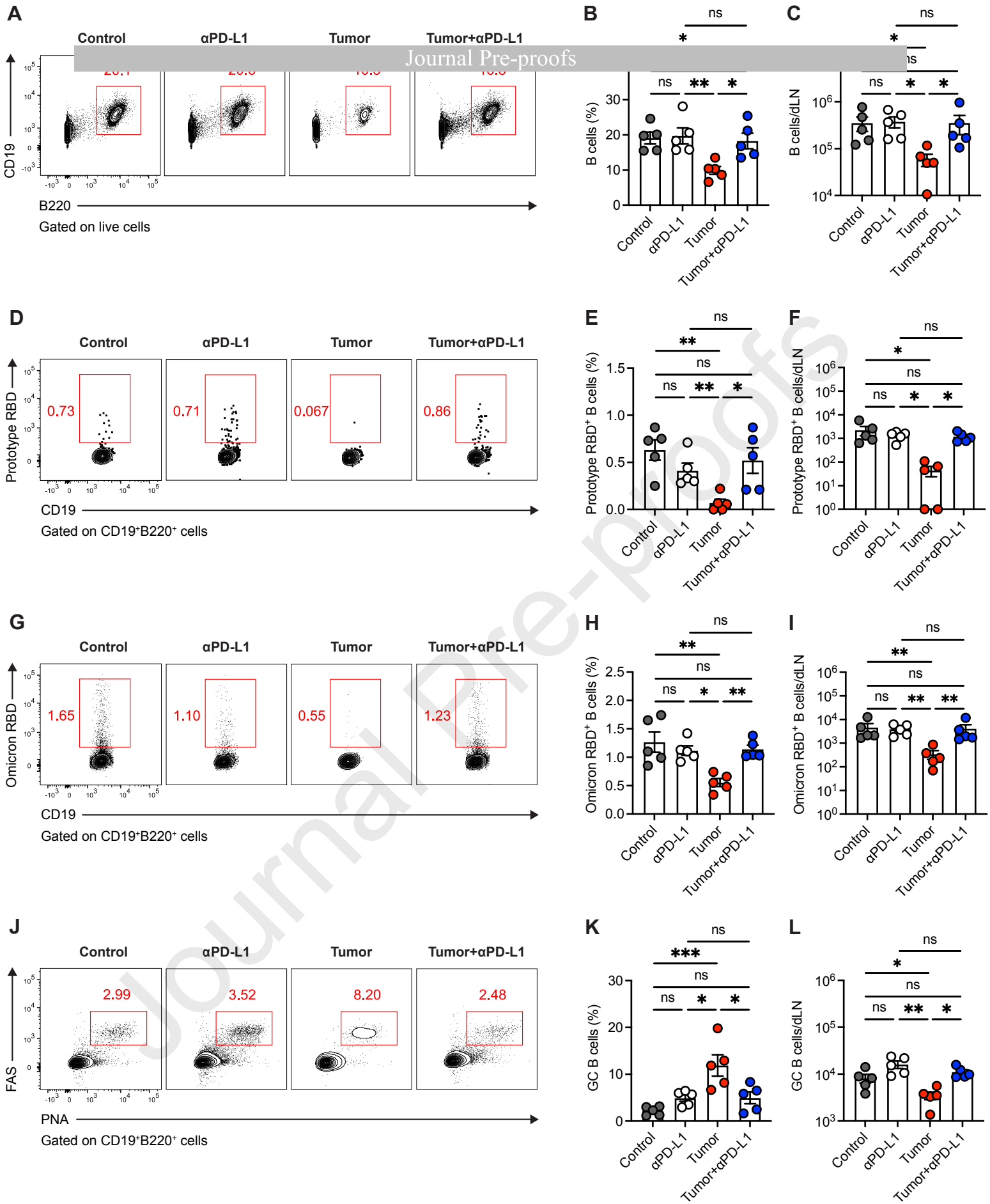

Figure 3

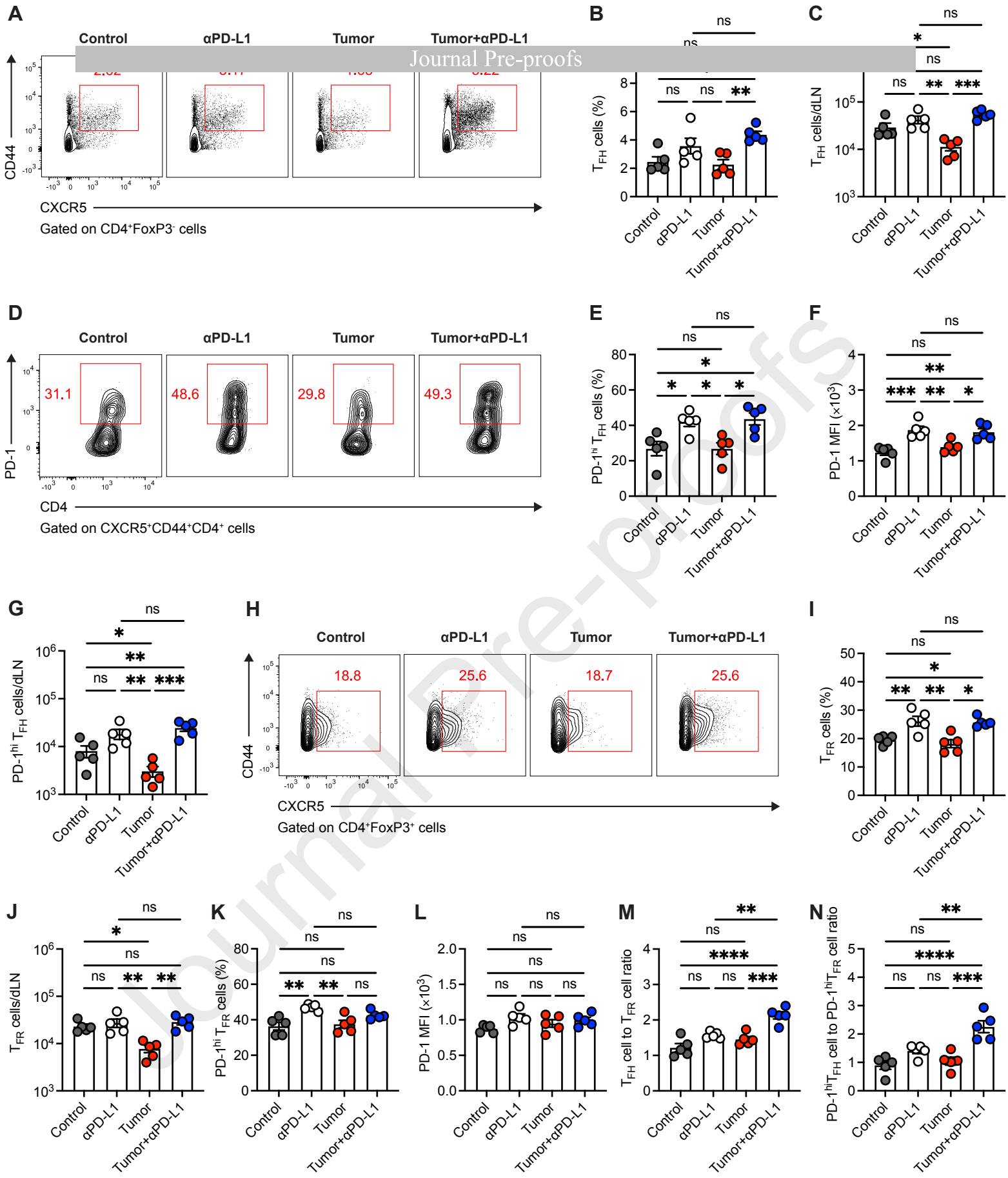

Figure 4

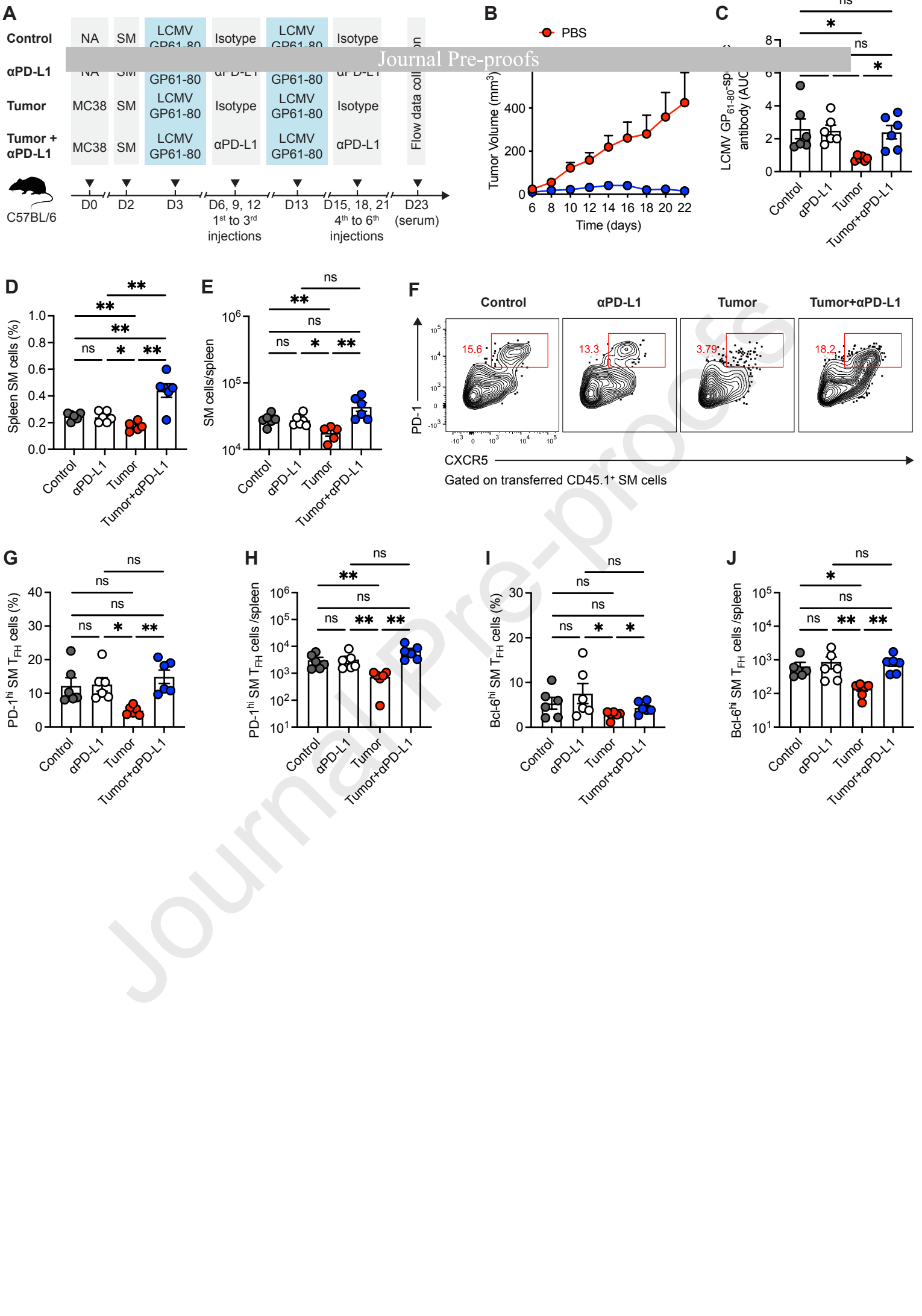

Figure 5